Supplement

Table S1: A list of ICOS stations, their land cover, their coordinates, the coordinates of the corresponding grid cell of the 3 km European CORDEX grid used in our simulations, and their number of 8-daily data points available for our analyses for ET and GPP. Note that stations that do not belong to PFT ENF, DBF, GRA, and CRO were omitted, and some included sites did not
1205 **have data corresponding with the study period (1995 - 2018), thus having a count of 0 data points. See Section 2.2.1. Stations, where the land cover was not directly indicated in the metadata sites were also left out in our analyses.**

ID	country	PFT	lat	lon	lat (cell)	lon (cell)	N (ET)	N (GPP)
BE-Bra	Belgium	ENF	51.31	4.52	51.29	4.51	503	670
BE-Dor	Belgium	GRA	50.31	4.97	50.31	4.96	0	270
BE-Lcr	Belgium	DBF	51.11	3.85	51.10	3.85	0	0
BE-Lon	Belgium	CRO	50.55	4.75	50.57	4.76	440	476
CH-Cha	Switzerland	GRA	47.21	8.41	47.21	8.43	386	459
CH-Dav	Switzerland	ENF	46.82	9.86	46.80	9.84	546	866
CH-Fru	Switzerland	GRA	47.12	8.54	47.11	8.53	260	447
CH-Oe2	Switzerland	CRO	47.29	7.73	47.28	7.72	0	592
CZ-BK1	Czech Republic	ENF	49.50	18.54	49.50	18.54	140	389
CZ-Lnz	Czech Republic	DBF	48.68	16.95	48.67	16.95	0	145
DE-Geb	Germany	CRO	51.10	10.91	51.10	10.93	797	638
DE-Gri	Germany	GRA	50.95	13.51	50.95	13.49	598	492
DE-Hai	Germany	DBF	51.08	10.45	51.07	10.45	754	548
DE-HoH	Germany	DBF	52.09	11.22	52.09	11.23	178	113
DE-Kli	Germany	CRO	50.89	13.52	50.90	13.54	404	450
DE-RuR	Germany	GRA	50.62	6.30	50.62	6.28	321	309
DE-RuS	Germany	CRO	50.87	6.45	50.86	6.44	232	224
DE-RuW	Germany	ENF	50.50	6.33	50.51	6.31	0	125
DE-Tha	Germany	ENF	50.96	13.57	50.96	13.58	935	888
DK-Gds	Denmark	ENF	56.07	9.33	56.07	9.34	0	0
DK-Sor	Denmark	DBF	55.49	11.64	55.48	11.65	379	882

FI-Hyy	Finland	ENF	61.85	24.29	61.86	24.29	373	812
FI-Ken	Finland	ENF	67.99	24.24	67.99	24.23	0	18
FI-Let	Finland	ENF	60.64	23.96	60.63	23.96	344	254
FI-Var	Finland	ENF	67.75	29.61	67.76	29.63	119	133
FR-Aur	France	CRO	43.55	1.11	43.54	1.12	389	483
FR-Bil	France	ENF	44.49	-0.96	44.50	-0.98	188	144
FR-FBn	France	ENF	43.24	5.68	43.25	5.69	0	358
FR-Fon	France	DBF	48.48	2.78	48.47	2.80	0	566
FR-Gri	France	CRO	48.84	1.95	48.86	1.95	397	313
FR-Hes	France	DBF	48.67	7.06	48.67	7.05	224	219
FR-Lam	France	CRO	43.50	1.24	43.51	1.25	439	431
FR-Tou	France	GRA	43.57	1.37	43.58	1.38	45	28
IT-BFt	Italy	DBF	45.20	10.74	45.21	10.75	0	0
IT-MBo	Italy	GRA	46.01	11.05	46.00	11.04	554	582
IT-Ren	Italy	ENF	46.59	11.43	46.58	11.44	466	525
IT-SR2	Italy	ENF	43.73	10.29	43.74	10.31	238	214
IT-Tor	Italy	GRA	45.84	7.58	45.85	7.57	333	251
RU-Fy2	Russia	ENF	56.45	32.90	56.46	32.89	146	138
SE-Htm	Sweden	ENF	56.10	13.42	56.10	13.42	171	152
SE-Nor	Sweden	ENF	60.09	17.48	60.09	17.50	216	181
SE-Svb	Sweden	ENF	64.26	19.77	64.26	19.77	138	109

Table S2: The RMSE and PBIAS for model ET in relation to the ICOS observations. Stations from ICOS that did not belong to PFT ENF, DBF, CRO, or GRA or did not have overlapping periods were omitted. See Section 2.4.2. For the amount of data points per station used for the calculations, see Table S1.

	ET RMSE [mm day^{-1}]					ET PBIAS [%]				
	CLM5$_{grid}$	CLM5$_{P}$ FT	ERA5L	GLASS	GLEAM	CLM5$_{grid}$	CLM5$_{P}$ FT	ERA5L	GLASS	GLEAM
BE-Bra	0.53	0.52	1.1	1.12	0.65	21.18	23.28	102.74	86.9	53.51
BE-Lon	0.65	0.99	0.92	0.83	0.48	13.44	24.31	67.7	44.85	20.31
CH-Cha	0.78	0.85	0.53	0.59	0.55	-32.31	-21.19	-13.4	-9.81	-8.37
CH-Dav	1.19	0.94	1.35	0.91	0.84	-50.35	-32.89	-54.06	-31.86	-27.21
CH-Fru	0.6	0.85	0.61	0.49	0.59	-23.14	-8.38	-6.73	-4.59	6.33
CZ-BK1	0.47	0.54	0.57	0.76	0.52	-23.38	-25.8	28.72	20.22	24.72
DE-Geb	0.51	0.83	0.86	0.71	0.48	-6.91	-5.24	64.07	40.18	14.67
DE-Gri	0.48	0.77	0.53	0.56	0.36	1.4	10.84	32.03	19.42	8.18
DE-Hai	0.48	0.6	0.75	0.72	0.5	1.23	7.5	54.25	42.96	27.83
DE-HoH	0.69	0.65	0.58	0.6	0.65	-27.75	-16.19	-1.24	-10.98	-24.17
DE-Kli	0.64	0.99	0.7	0.74	0.58	3.53	16.23	36.42	24.16	20.33
DE-RuR	0.4	0.77	0.53	0.6	0.45	-18.28	5.14	27.41	9.26	16.76
DE-RuS	0.79	0.98	0.49	0.64	0.69	-35.1	-32.57	4.96	-15.5	-27.25
DE-Tha	0.61	0.49	0.69	0.71	0.47	0.03	-0.58	39.24	20.32	13.76
DK-Sor	0.6	0.59	0.65	0.55	0.5	-25.3	-14.11	40.06	19.22	2.01
FI-Hyy	0.5	0.52	0.41	0.49	0.63	-35.03	-26.83	20.28	11.59	41.51
FI-Let	0.67	0.62	0.78	0.61	0.71	-32.63	-21.82	48.73	9.52	38.69
FI-Var	0.37	0.48	0.46	0.69	0.59	-34.03	-14.31	65.47	55.65	85.29
FR-Aur	0.81	1.18	1.03	1.08	0.75	6.82	47.61	54.17	39.04	18.56
FR-Bil	0.67	0.9	0.7	1.5	0.68	-25.39	-27.73	23.93	50.29	24.77
FR-Gri	0.76	1	0.77	0.85	0.55	-7.41	-2.62	38.22	22.79	-1.57
FR-Hes	0.58	0.67	0.86	0.83	0.72	0.92	13.76	52.3	36.7	36.96

61

FR-Lam	0.85	1.09	0.98	0.96	0.78	-8.52	19.85	29.34	15.93	-3.31
FR-Tou	0.7	0.9	1.05	0.87	0.5	-35.79	-45.8	61.12	31.2	17.87
IT-MBo	0.53	0.8	0.46	0.48	0.7	-2.52	-17.37	8.64	6.11	15.84
IT-Ren	0.86	0.82	0.71	0.76	0.75	-25.41	-5.21	-11.11	-17.11	-0.6
IT-SR2	0.91	1.56	0.76	0.71	0.81	-33.93	-60.78	28.67	4.92	-23.63
IT-Tor	1.03	1.14	0.87	0.65	0.84	-43.24	-46.1	-35.9	-11.77	-29.23
RU-Fy2	0.41	0.51	0.69	0.65	0.67	-3.69	-16.07	52.22	25.24	52.85
SE-Htm	0.45	0.45	0.89	1.18	0.9	-7.53	-3.65	72.62	60.16	77.51
SE-Nor	0.36	0.37	0.57	0.66	0.58	-15.2	-5.08	46.5	21.54	45.74
SE-Svb	0.46	0.6	0.33	0.52	0.56	-22.3	-4.25	14.62	14.77	33.97

1215

Table S3: The RMSE and PBIAS for model GPP in relation to the ICOS observations. Stations from ICOS that did not belong to PFT ENF, DBF, CRO, or GRA or did not have overlapping periods were omitted. See Section 2.4.2. For the amount of data points per station used for the calculations, see Table S1.

	GPP RMSE [g C day^{-1}]			GPP PBIAS [%]		
	CLM5$_{grid}$	CLM5$_{PFT}$	GLASS	CLM5$_{grid}$	CLM5$_{PFT}$	GLASS
BE-Bra	2.29	1.69	1.3	-35.31	0.58	4.7
BE-Dor	3.19	3.39	2.74	-41.65	-40.27	-35.08
BE-Lon	4.31	4.31	3.98	-18.12	-8.2	-11.27
CH-Cha	4.61	3.94	4.29	-50.85	-38.48	-47.12
CH-Dav	2.4	2.13	2.13	-16.6	30.76	-25.06
CH-Fru	3.6	2.84	2.62	-39.95	-23.07	-23.89
CH-Oe2	3.75	3.95	3.53	-10.63	-12.43	2.68
CZ-BK1	2.79	2.31	1.95	-37.01	-22.8	-20.62
CZ-Lnz	4.64	3.44	2.9	-61.65	-48.99	-28.72
DE-Geb	3.63	4.32	2.98	-35.47	-39.88	-1.82
DE-Gri	2.61	2.68	2.02	-21.13	-11.9	-9.62
DE-Hai	2.83	2.59	1.7	-34.4	-41.98	-1.49
DE-HoH	2.94	2.51	3.04	-30.18	-40.09	-27.51
DE-Kli	3.5	3.66	3.15	1.73	2.03	-2.71
DE-RuR	2.4	2.39	2	-26.97	-10.45	-19.49
DE-RuS	4.74	5.05	4.34	-43.33	-45.5	-34.54
DE-RuW	2.63	2.61	2.14	-32.06	-27.58	-23.83
DE-Tha	1.87	1.48	1.29	-28.94	-3.95	-19.24
DK-Sor	4.39	4.07	3.21	-47.92	-49.59	-35.2
FI-Hyy	1.3	1.29	0.81	-14.86	-0.32	-8.87
FI-Ken	1.16	2.34	0.72	-2.71	53.03	-13.93
FI-Let	2.05	2.02	1.53	-19.04	-4.69	-19.86
FI-Var	1.4	3.22	0.89	58.88	155.55	20.97

FR-Aur	3.28	4.05	3.25	9.34	68.22	8.98
FR-Bil	1.75	2.23	1.67	-24.81	-24.43	-0.67
FR-FBn	2.38	3.73	1.82	-48.88	-77.01	15.32
FR-Fon	3.1	2.87	2.74	-26.88	-36.12	-21.86
FR-Gri	4.16	4.24	3.73	-18.64	-13.82	-15.47
FR-Hes	3.7	3.24	3.32	-24.24	-35.9	-17.18
FR-Lam	3.91	4.5	3.95	-4.08	44.74	-8.86
FR-Tou	3.44	2.53	1.77	-73.37	-47.07	-10.42
IT-MBo	2.42	2.89	1.84	-7.88	-31.82	3.25
IT-Ren	1.53	2.32	1.77	11.56	33.15	-2.03
IT-SR2	5.12	6.78	4.07	-67.17	-88.85	-53.94
IT-Tor	1.82	2.49	1.66	-0.73	1.01	1.16
RU-Fy2	2.63	2.84	1.93	-26.01	-22.21	-23.36
SE-Htm	2.74	2.24	1.95	-38.02	-25.41	-26.83
SE-Nor	1.59	1.37	1.35	-25.47	-3.78	-21.52
SE-Svb	1.13	2.02	1.22	5.6	24.88	-24.05
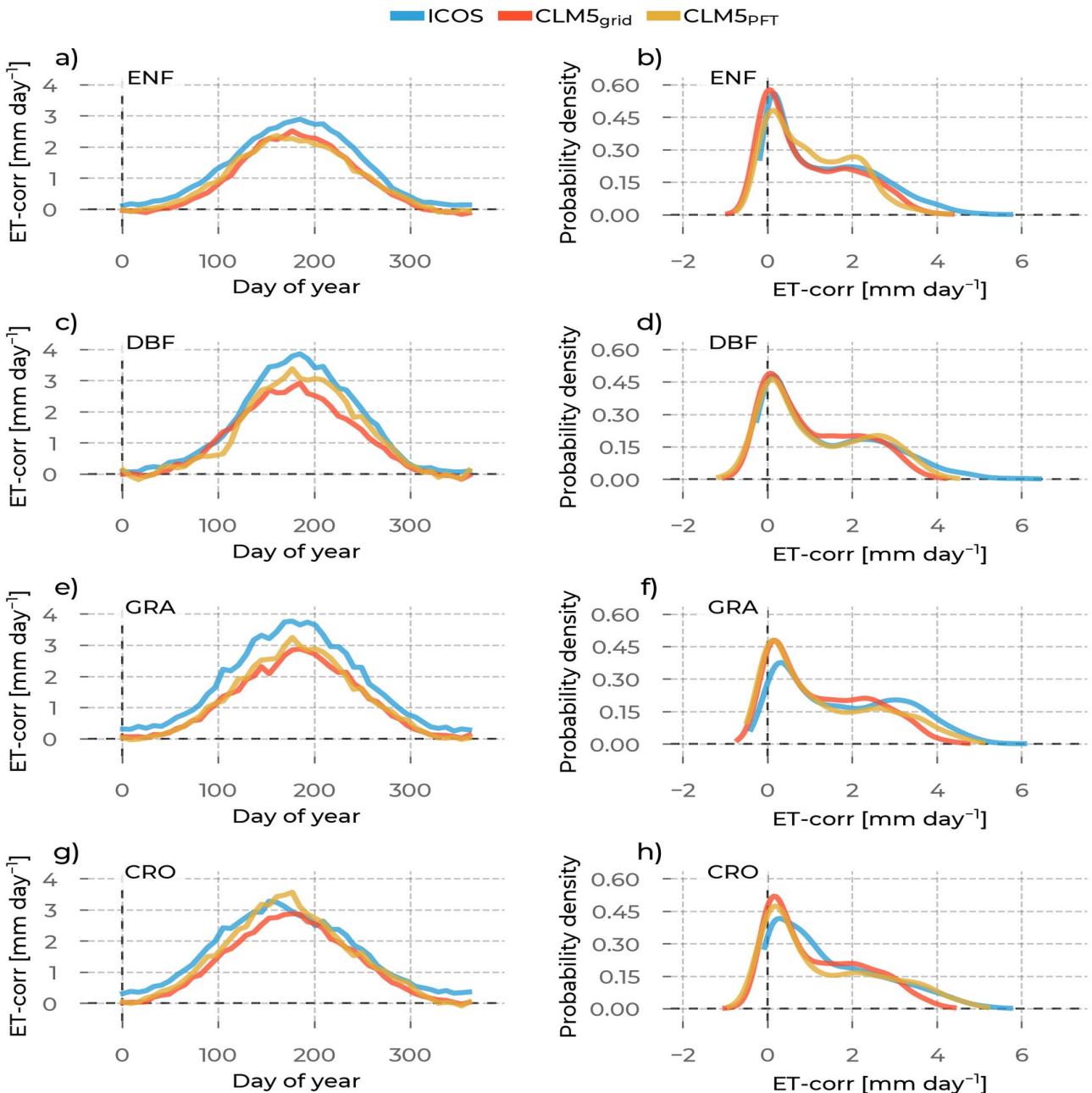
Figure S1: In the left column are the yearly energy balance corrected evapotranspiration (ET-corr) evolutions averaged across stations belonging to one PFT (rows). We differentiate the data source by color (ICOS observations: blue, CLM5_grid: red, CLM5_PFT: yellow, GLASS: green, ERA5L: brown, GLEAM: purple). The probability density curves for all ET-corr values from

1225 **stations belonging to the selected PFT are in the right column. Each row shows these plots for one PFT: Evergreen Needleleaf Forest (ENF), Deciduous Broadleaf Forest (DBF), Grasslands (GRA), and Croplands (CRO).**
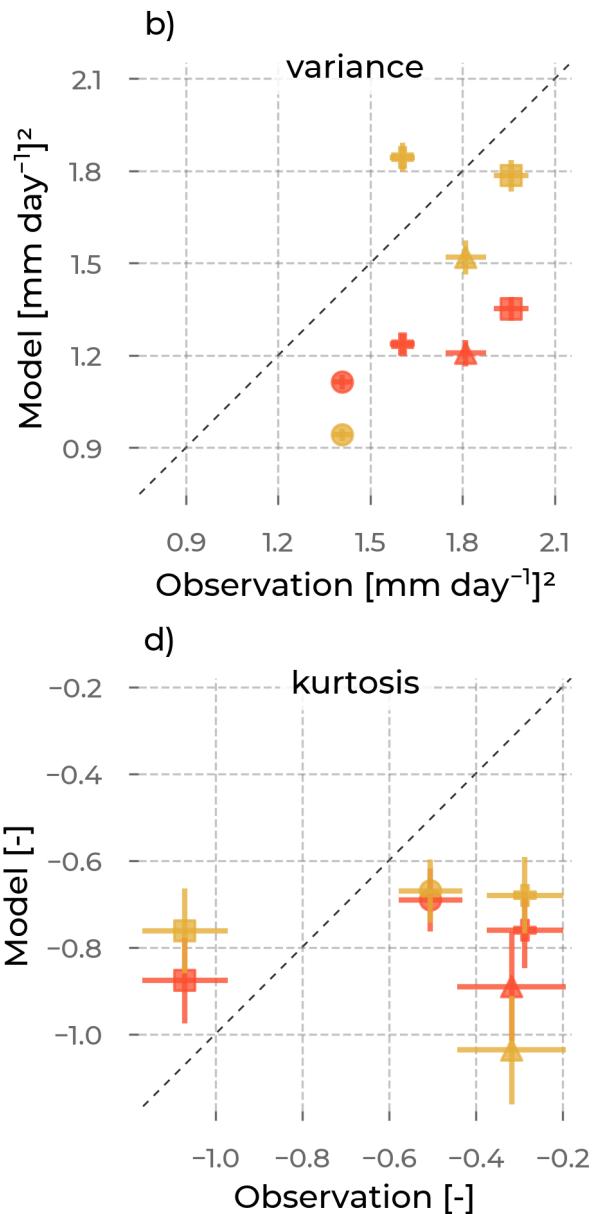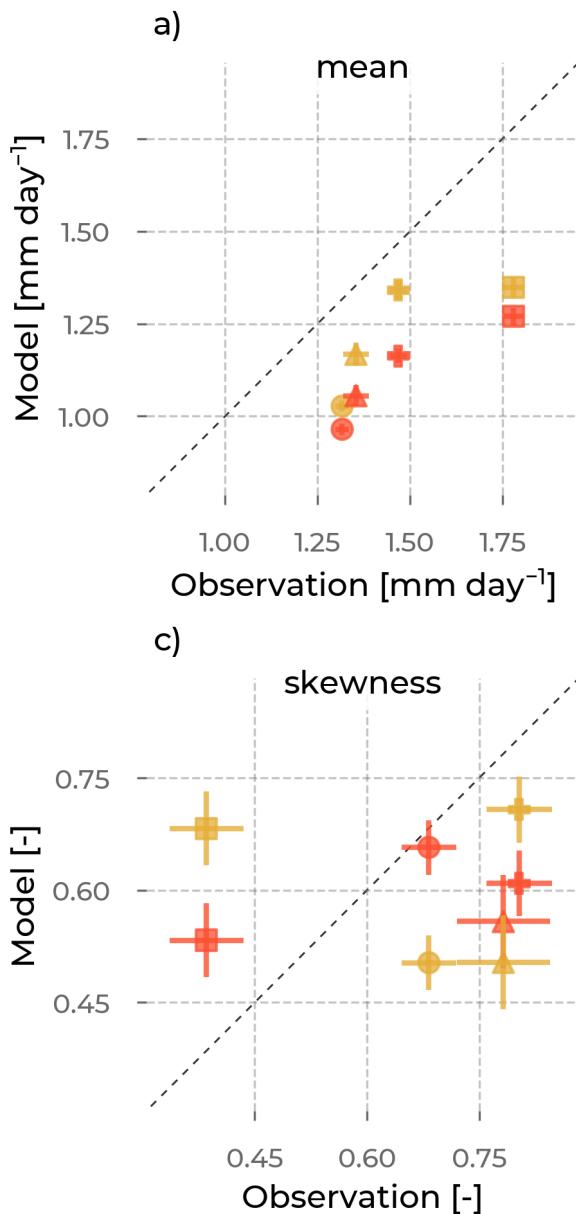
Figure S2: The mean (a), variance (b), skewness (c), and kurtosis (d) of the ET-corr distributions from the models (color, y-axis), as opposed to the corresponding values from observations (x-axis) aggregated for each PFT (marker type): Evergreen Needleleaf Forest (ENF), Deciduous Broadleaf Forest (DBF), Grasslands (GRA), Croplands (CRO). The error bars are the standard errors of the respective moment, depending on the sample size.
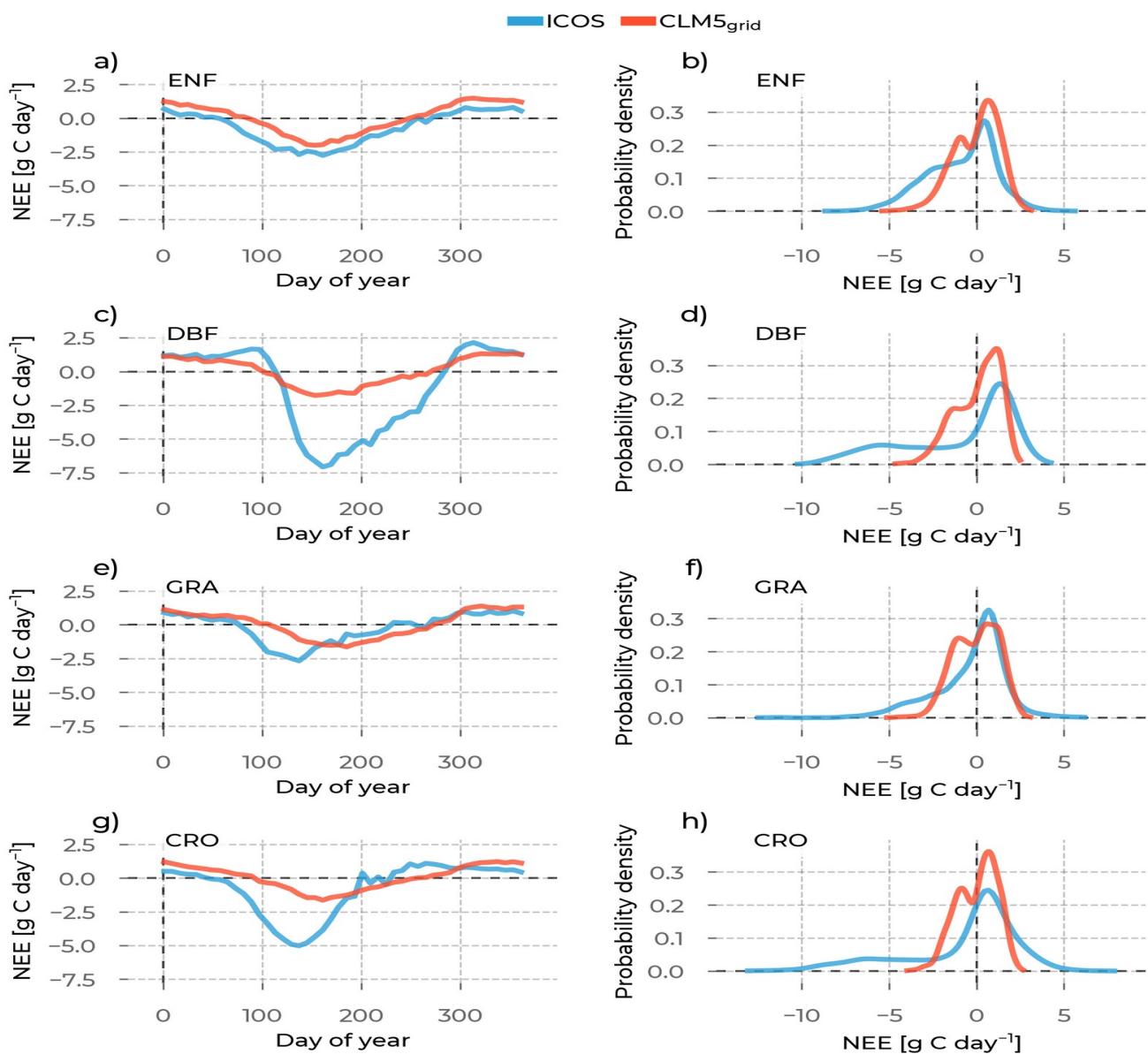
Figure S3: In the left column are the yearly net ecosystem exchange (NEE) evolutions averaged across stations belonging to one PFT (rows). We differentiate the data source by color (ICOS observations: blue, CLM5$_{grid}$: red, CLM5$_{PFT}$: yellow, GLASS: green, ERA5L: brown, GLEAM: purple). The probability density curves for all NEE values from stations belonging to the selected PFT are in the right column. Each row shows these plots for one PFT: Evergreen Needleleaf Forest (ENF), Deciduous Broadleaf Forest (DBF), Grasslands (GRA), and Croplands (CRO).
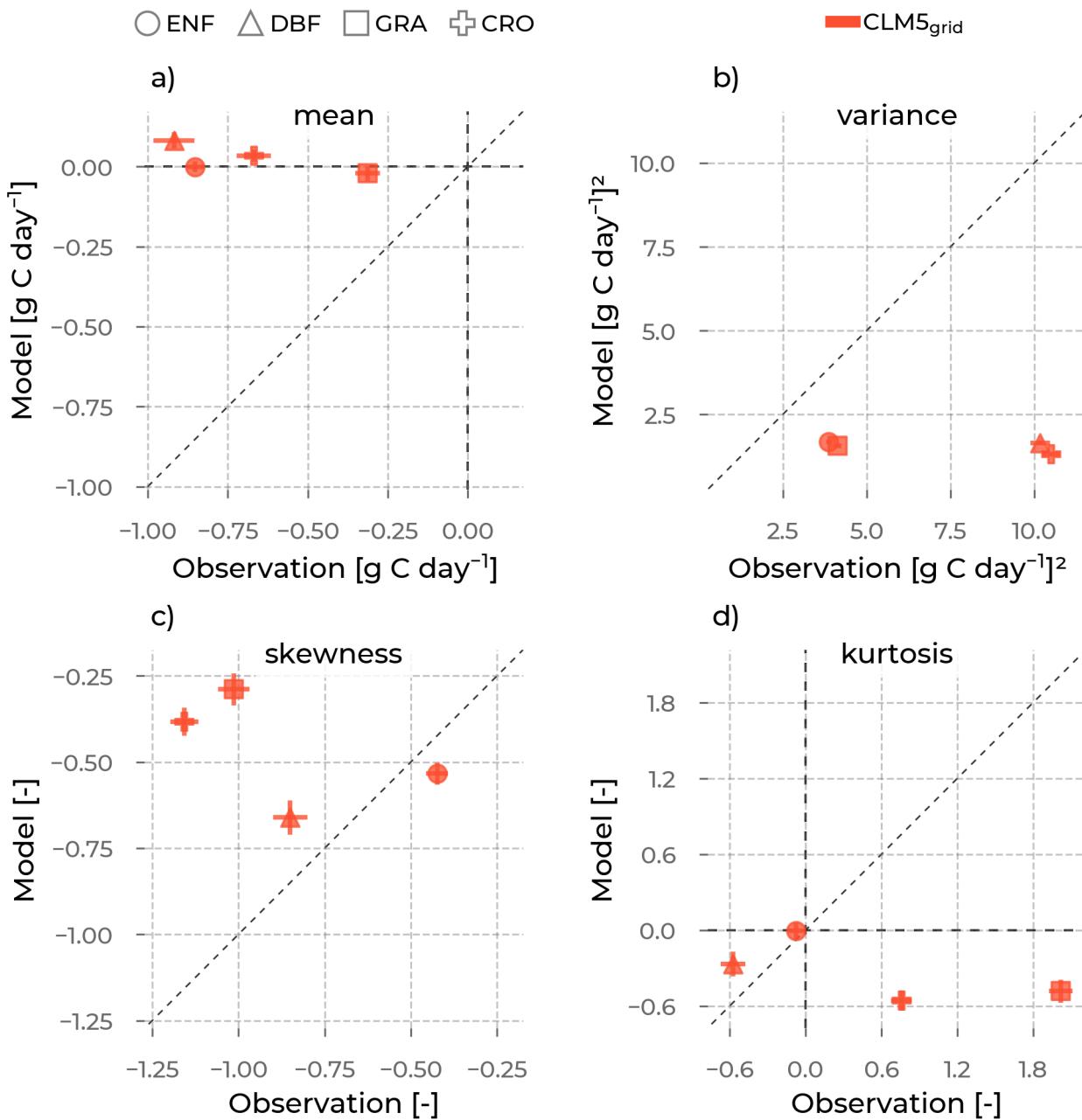
Figure S4: The mean (a), variance (b), skewness (c), and kurtosis (d) of the NEE distributions from the models (color, y-axis), as opposed to the corresponding values from observations (x-axis) aggregated for each PFT (marker type): Evergreen Needleleaf Forest (ENF), Deciduous Broadleaf Forest (DBF), Grasslands (GRA), Croplands (CRO). The error bars are the standard errors of the respective moment, depending on the sample size.

1245
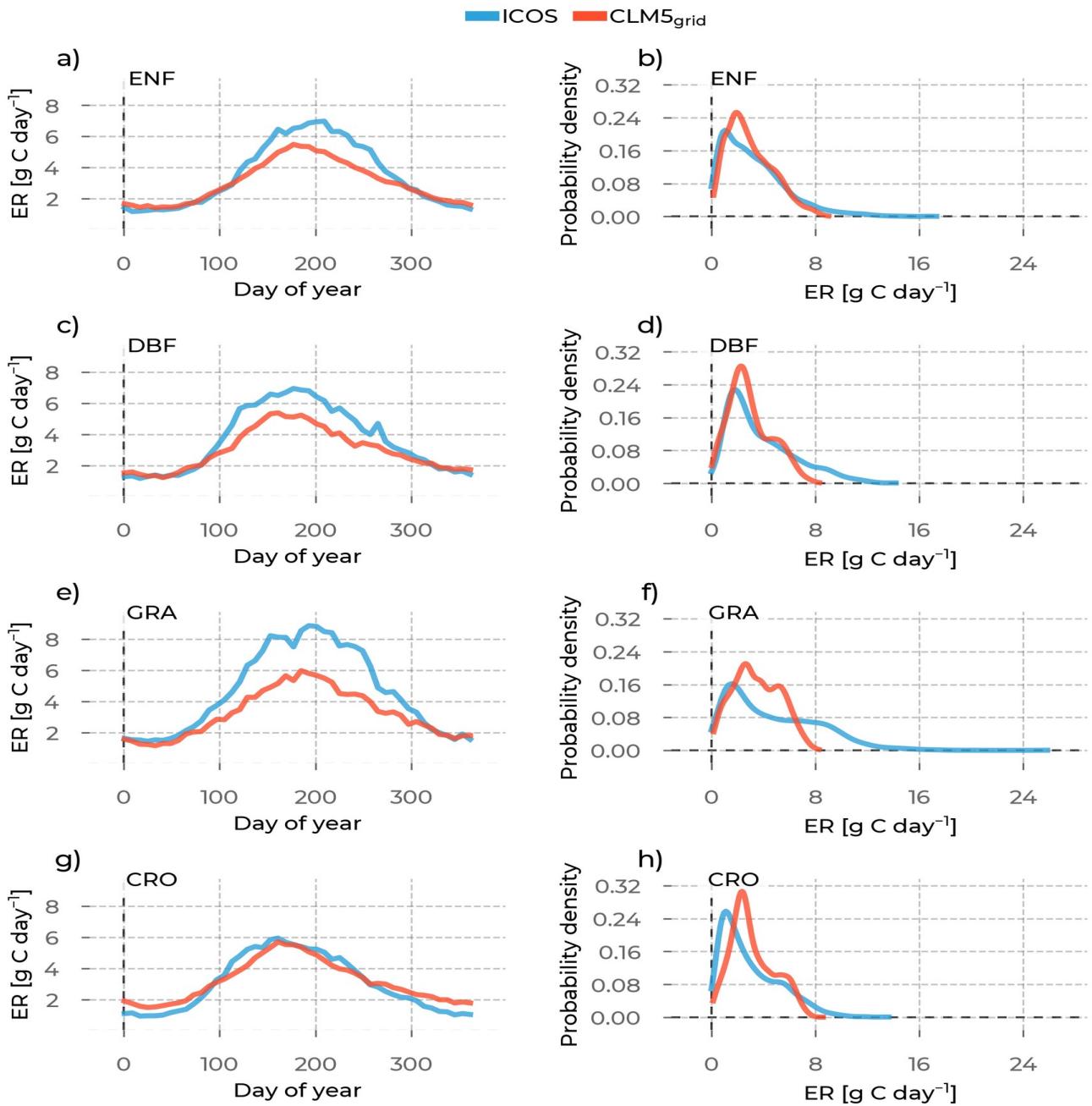
Figure S5: In the left column are the yearly ecosystem respiration (ER) evolutions averaged across stations belonging to one PFT (rows). We differentiate the data source by color (ICOS observations: blue, CLM5$_{grid}$: red, CLM5$_{PFT}$: yellow, GLASS: green, ERA5L: brown, GLEAM: purple). The probability density curves for all ER values from stations belonging to the selected

PFT are in the right column. Each row shows these plots for one PFT: Evergreen Needleleaf Forest (ENF), Deciduous Broadleaf Forest (DBF), Grasslands (GRA), and Croplands (CRO).
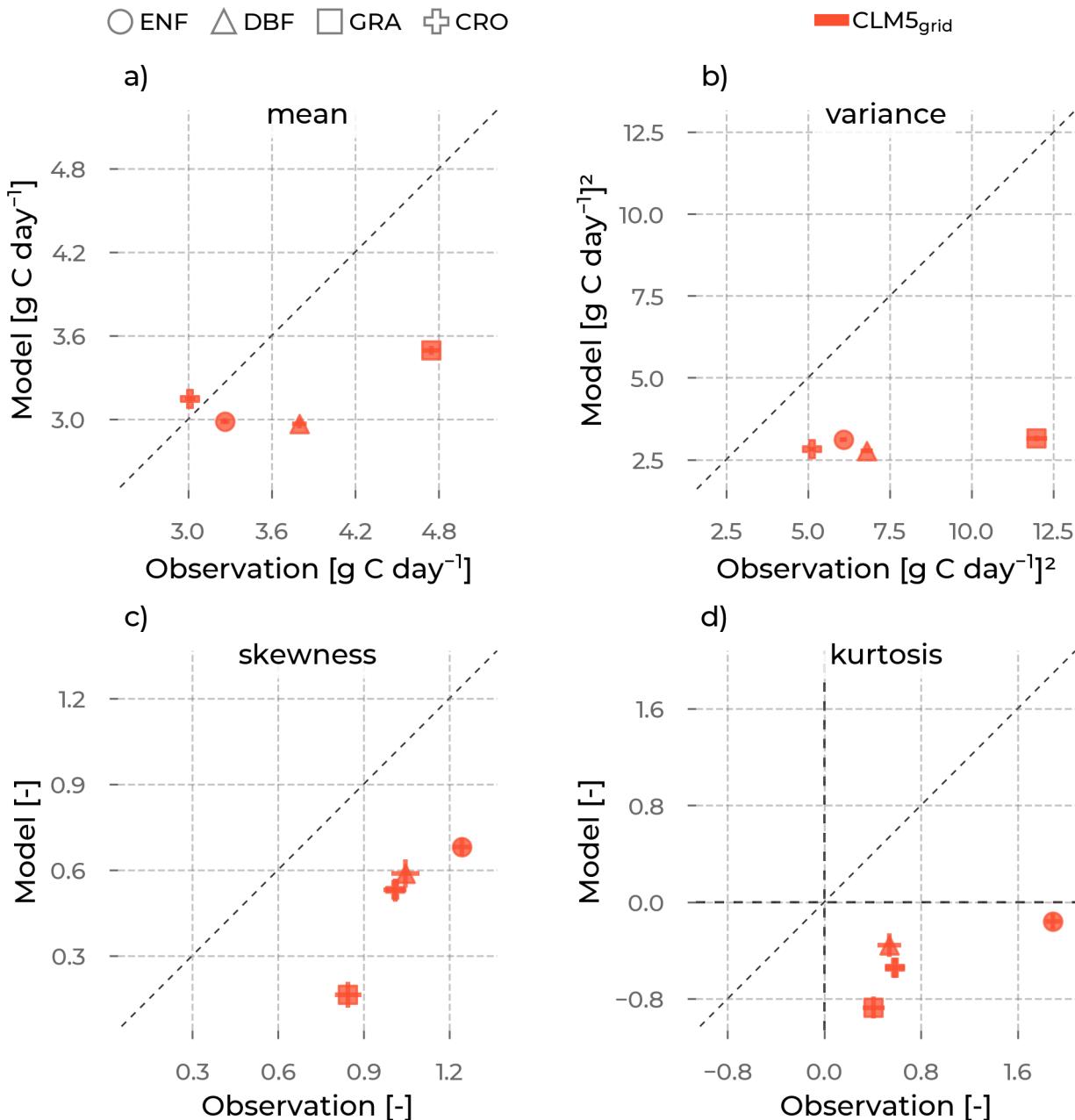
Figure S6: The mean (a), variance (b), skewness (c), and kurtosis (d) of the ER distributions from the models (color, y-axis), as opposed to the corresponding values from observations (x-

1260
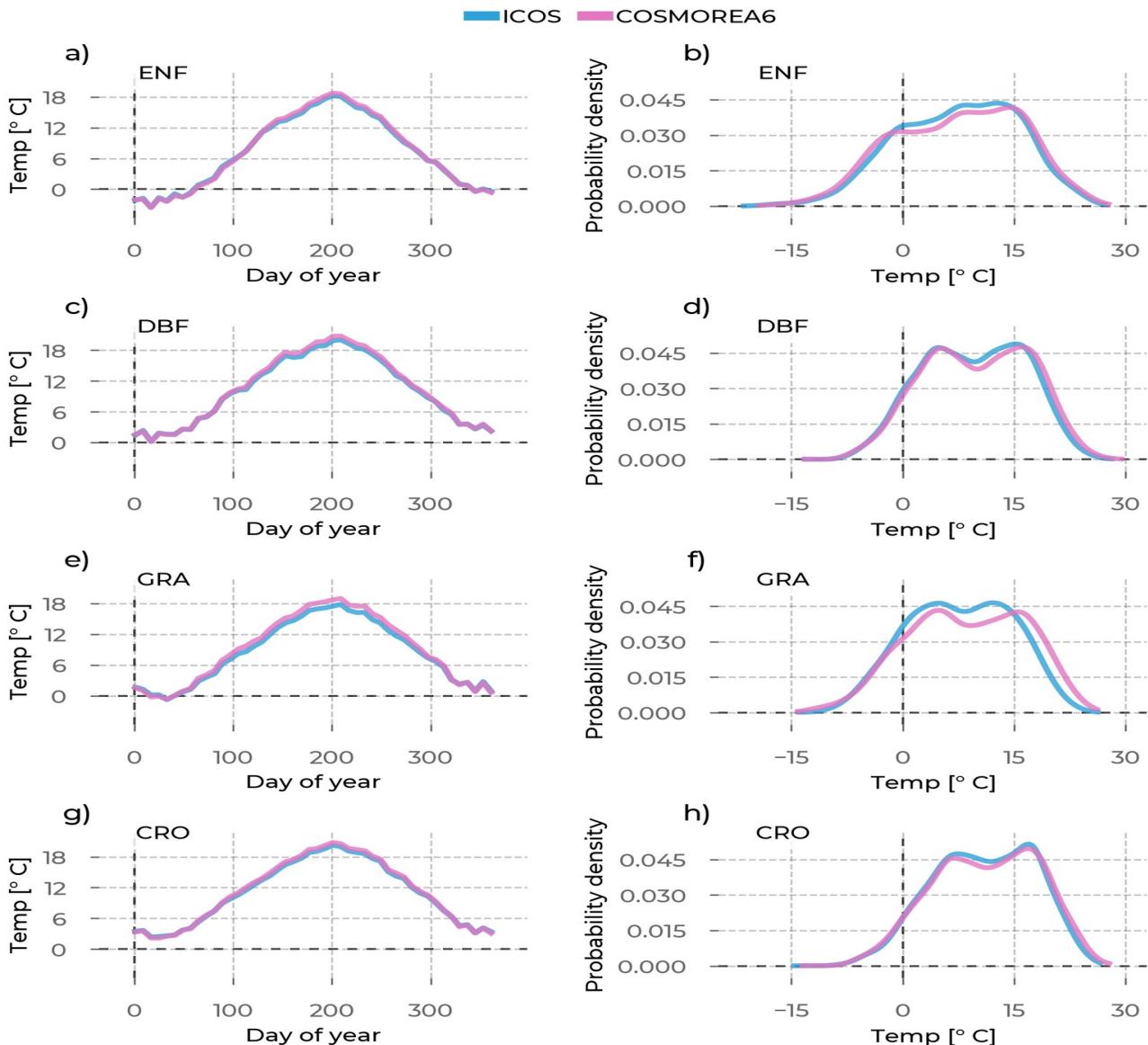
Figure S7: In the left column are the yearly Temperature (Temp) evolutions averaged across stations belonging to one PFT (rows). We differentiate the data source by color (ICOS observations: blue, CLM5$_{grid}$: red, CLM5$_{PFT}$: yellow, GLASS: green, ERA5L: brown, GLEAM: purple). The probability density curves for all Temp values from stations belonging to the selected PFT are in the right column. Each row shows these plots for one PFT: Evergreen

72

Needleleaf Forest (ENF), Deciduous Broadleaf Forest (DBF), Grasslands (GRA), and Croplands (CRO).
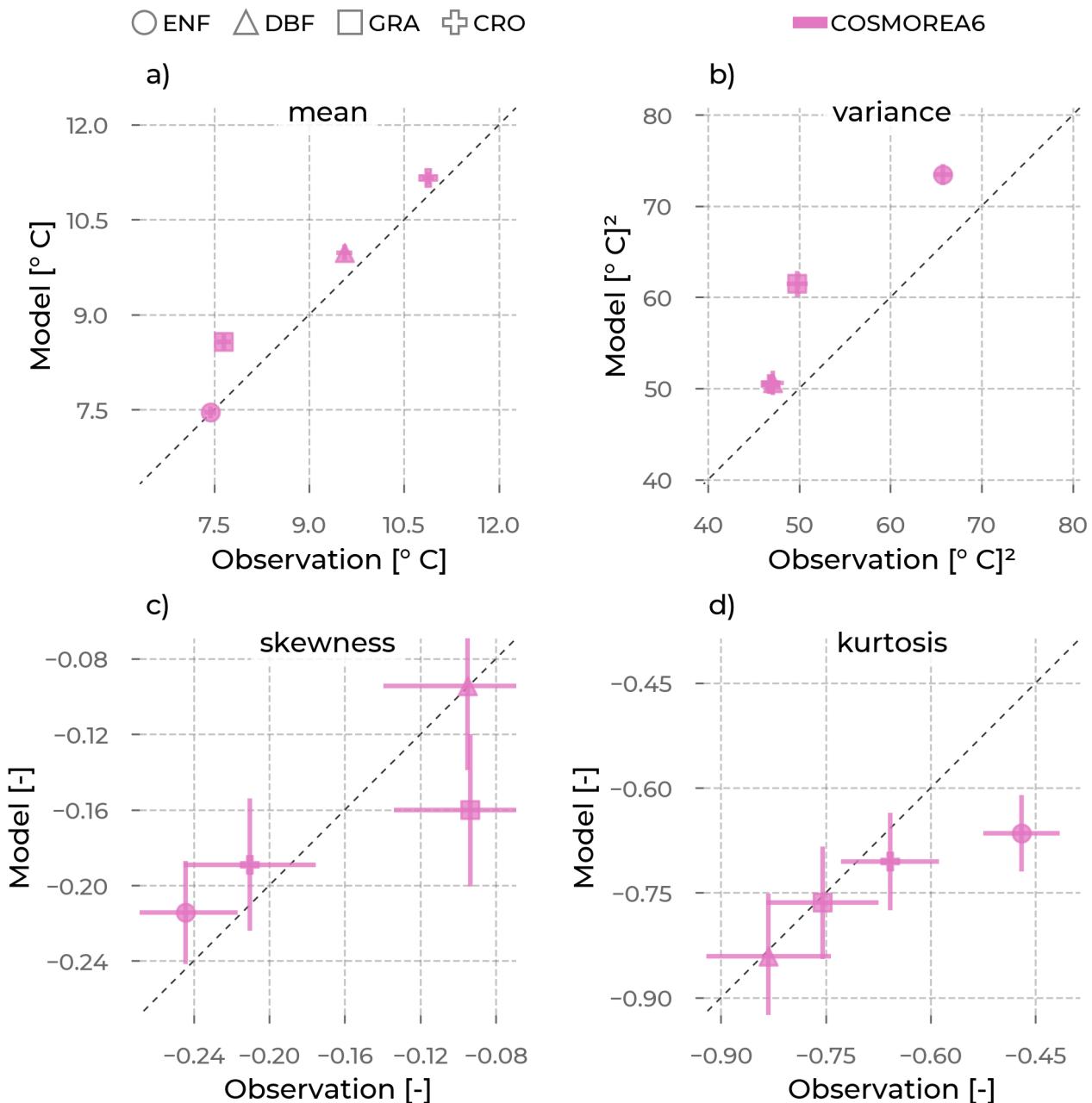
Figure S8: The mean (a), variance (b), skewness (c), and kurtosis (d) of the Temp distributions from the models (color, y-axis), as opposed to the corresponding values from observations (x-

axis) aggregated for each PFT (marker type): Evergreen Needleleaf Forest (ENF), Deciduous Broadleaf Forest (DBF), Grasslands (GRA), Croplands (CRO). The error bars are the standard errors of the respective moment, depending on the sample size.

1275
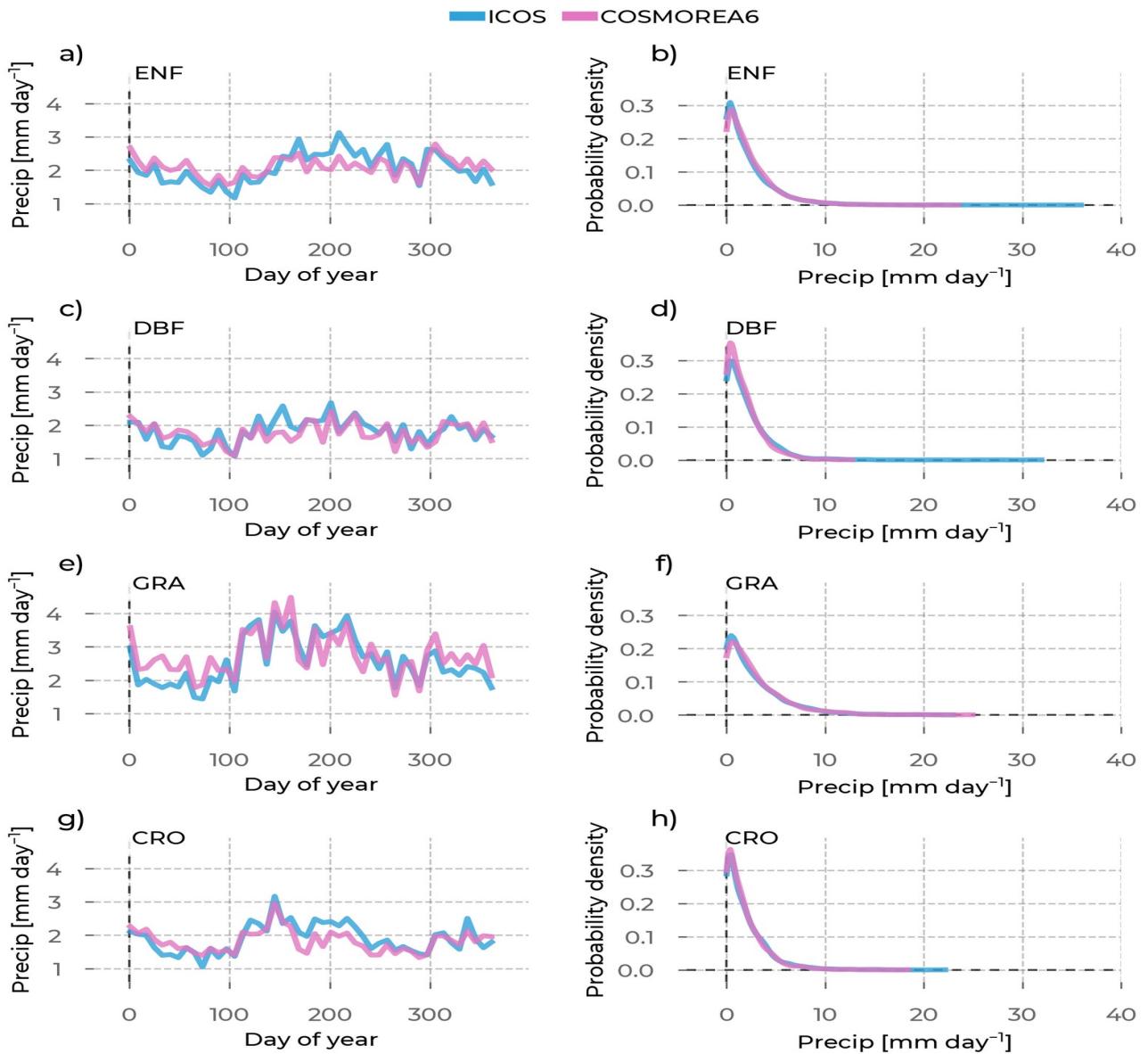
Figure S9: In the left column are the yearly Precipitation (Precip) evolutions averaged across stations belonging to one PFT (rows). We differentiate the data source by color (ICOS observations: blue, CLM5$_{grid}$: red, CLM5$_{PFT}$: yellow, GLASS: green, ERA5L: brown, GLEAM: purple). The probability density curves for all Precip values from stations belonging to the

1280 **selected PFT are in the right column. Each row shows these plots for one PFT: Evergreen Needleleaf Forest (ENF), Deciduous Broadleaf Forest (DBF), Grasslands (GRA), and Croplands (CRO).**
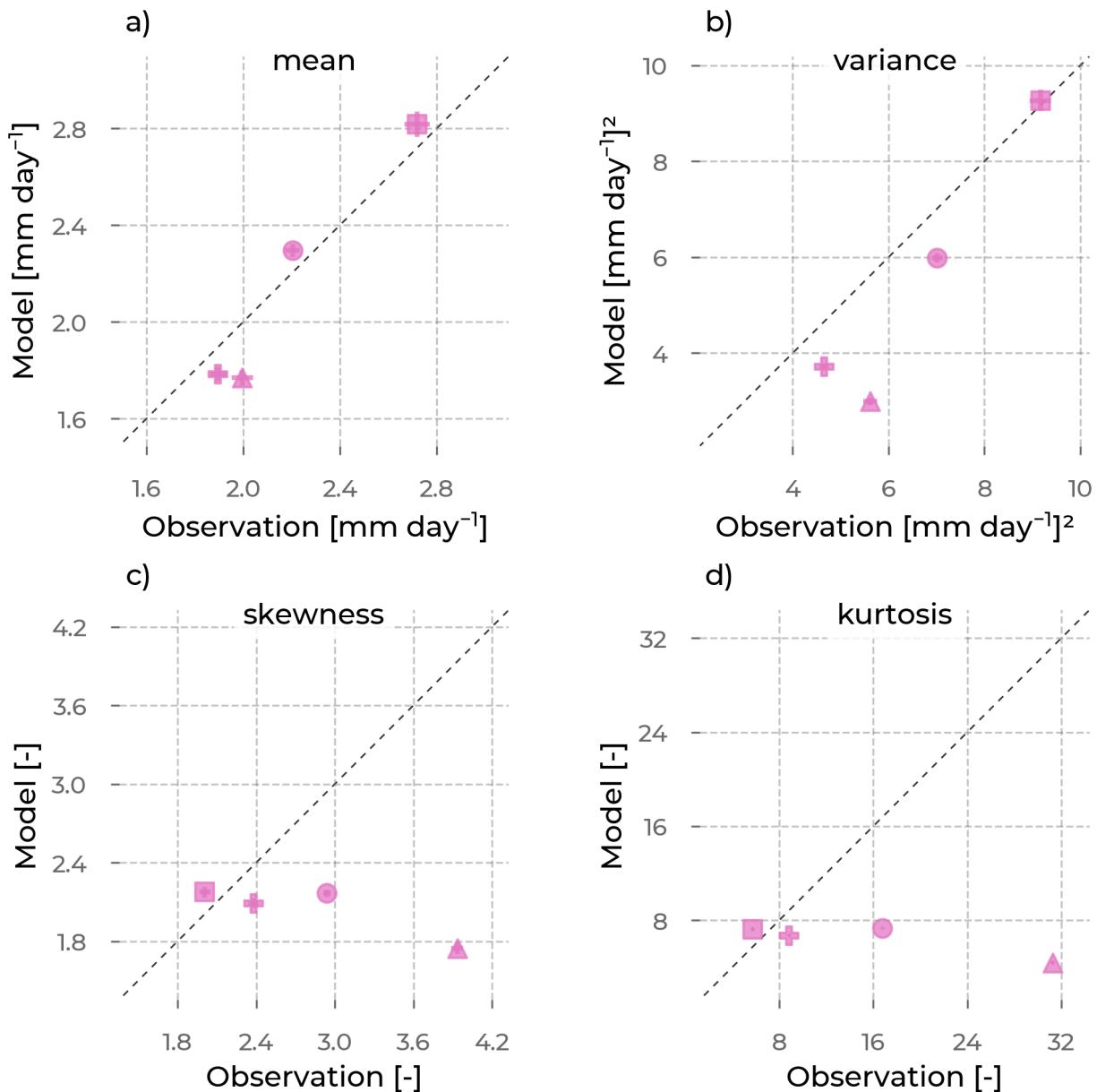
Figure S10: The mean (a), variance (b), skewness (c), and kurtosis (d) of the Precip distributions from the models (color, y-axis), as opposed to the corresponding values from observations (x-axis) aggregated for each PFT (marker type): Evergreen Needleleaf Forest (ENF), Deciduous Broadleaf Forest (DBF), Grasslands (GRA), Croplands (CRO). The error bars are the standard errors of the respective moment, depending on the sample size.
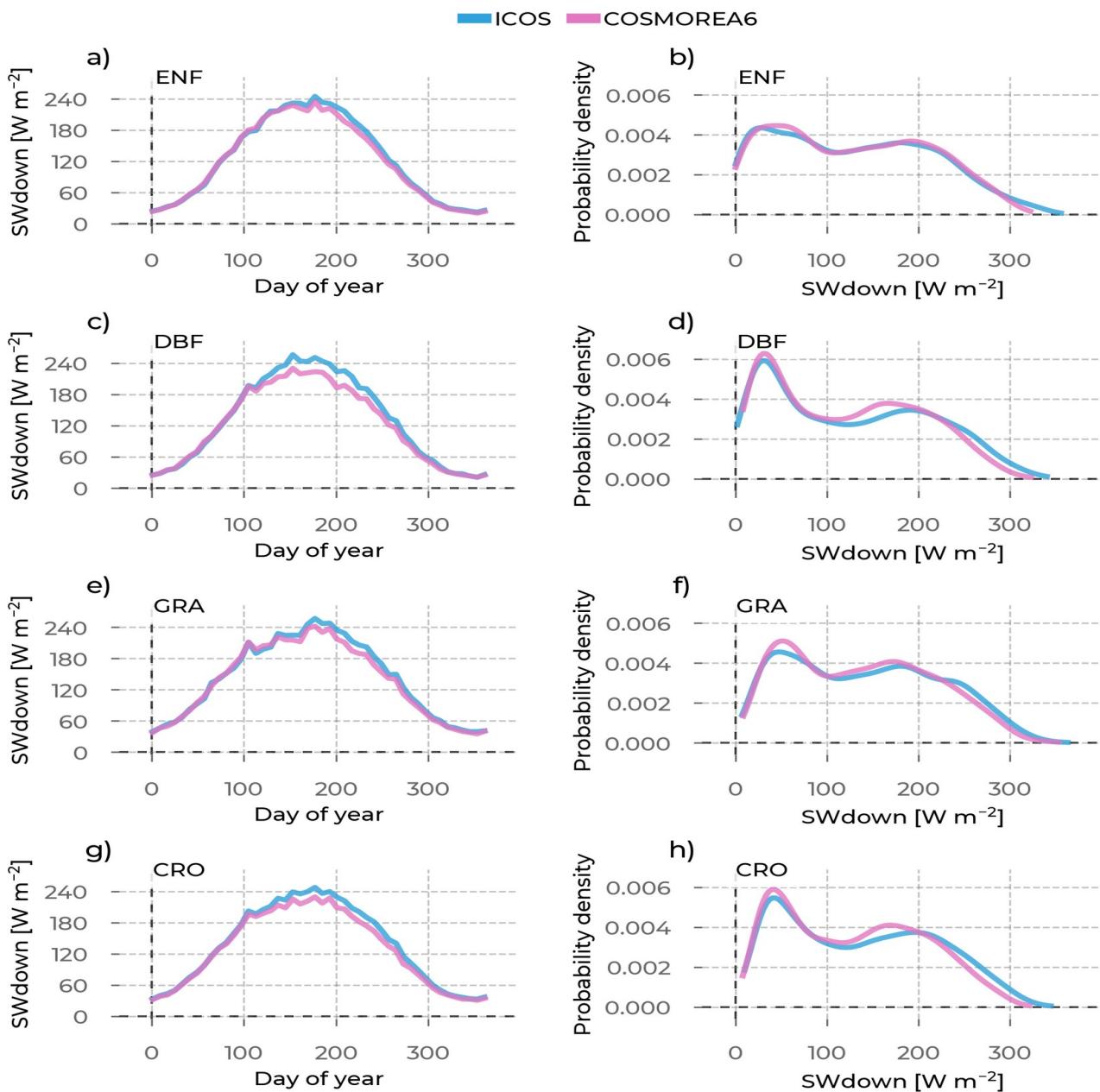
 Figure S11: In the left column are the yearly shortwave downward radiation (SWdown) evolutions averaged across stations belonging to one PFT (rows). We differentiate the data source by color (ICOS observations: blue, CLM5$_{grid}$: red, CLM5$_{PFT}$: yellow, GLASS: green, ERA5L: brown, GLEAM: purple). The probability density curves for all SWdown values from stations belonging to the selected PFT are in the right column. Each row shows these plots for

one PFT: Evergreen Needleleaf Forest (ENF), Deciduous Broadleaf Forest (DBF), Grasslands (GRA), and Croplands (CRO).
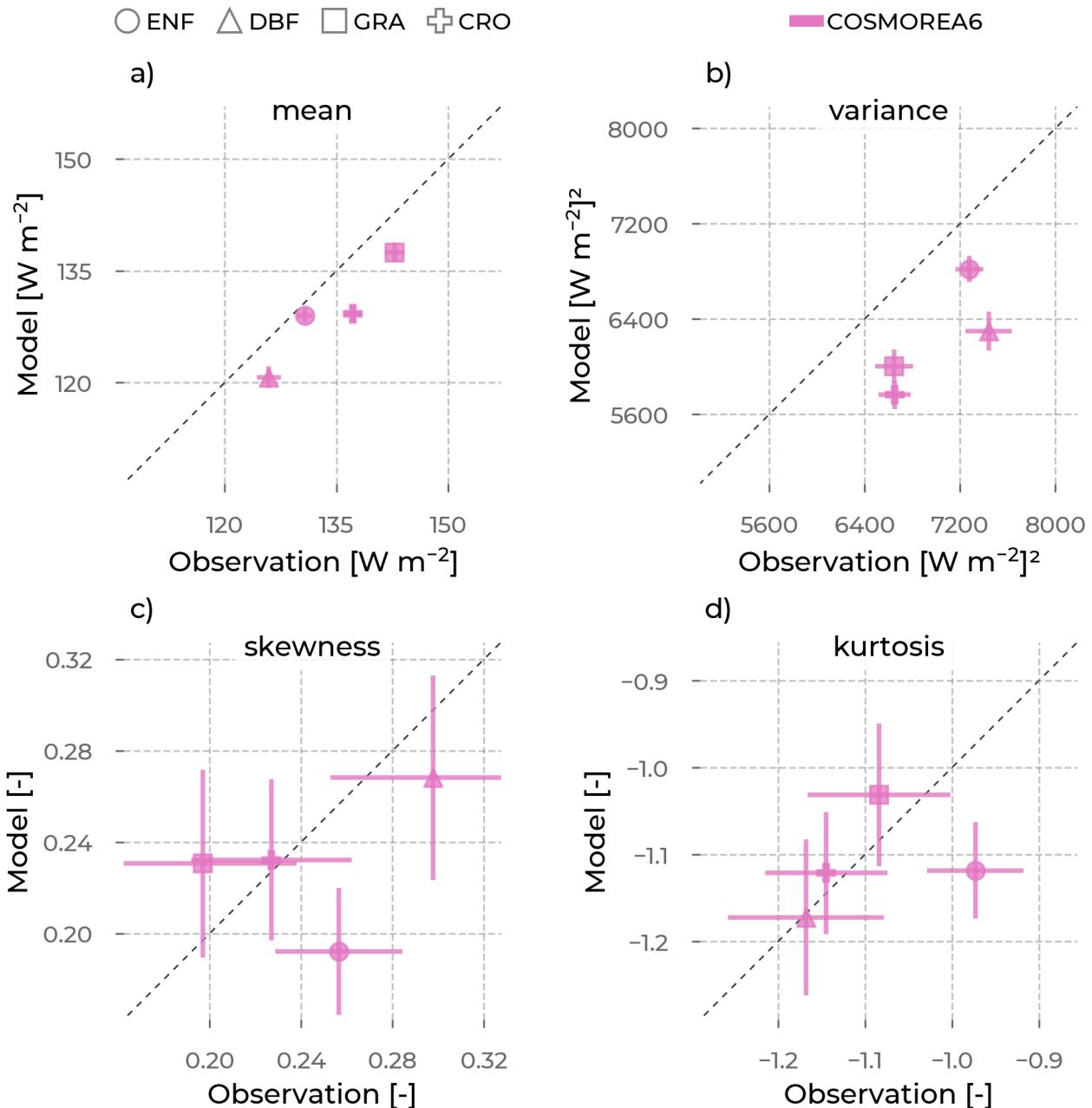
Figure S12: The mean (a), variance (b), skewness (c), and kurtosis (d) of the SWdown distributions from the models (color, y-axis), as opposed to the corresponding values from

1300 **observations (x-axis) aggregated for each PFT (marker type): Evergreen Needleleaf Forest (ENF), Deciduous Broadleaf Forest (DBF), Grasslands (GRA), Croplands (CRO). The error bars are the standard errors of the respective moment, depending on the sample size.**
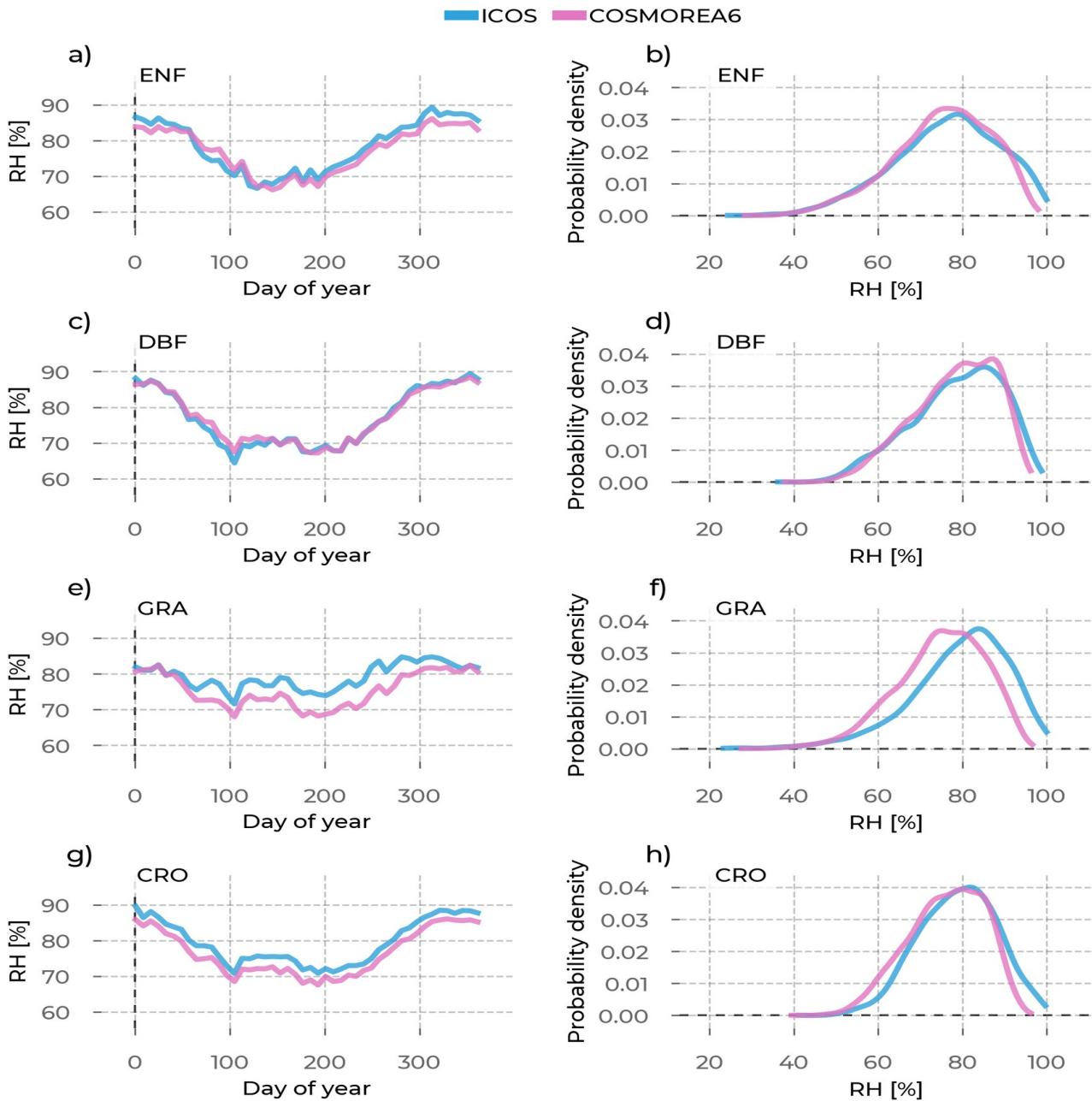
Figure S13: In the left column are the yearly relative humidity (RH) evolutions averaged across
stations belonging to one PFT (rows). We differentiate the data source by color (ICOS
observations: blue, CLM5$_{grid}$: red, CLM5$_{PFT}$: yellow, GLASS: green, ERA5L: brown, GLEAM:
purple). The probability density curves for all RH values from stations belonging to the selected

PFT are in the right column. Each row shows these plots for one PFT: Evergreen Needleleaf Forest (ENF), Deciduous Broadleaf Forest (DBF), Grasslands (GRA), and Croplands (CRO).
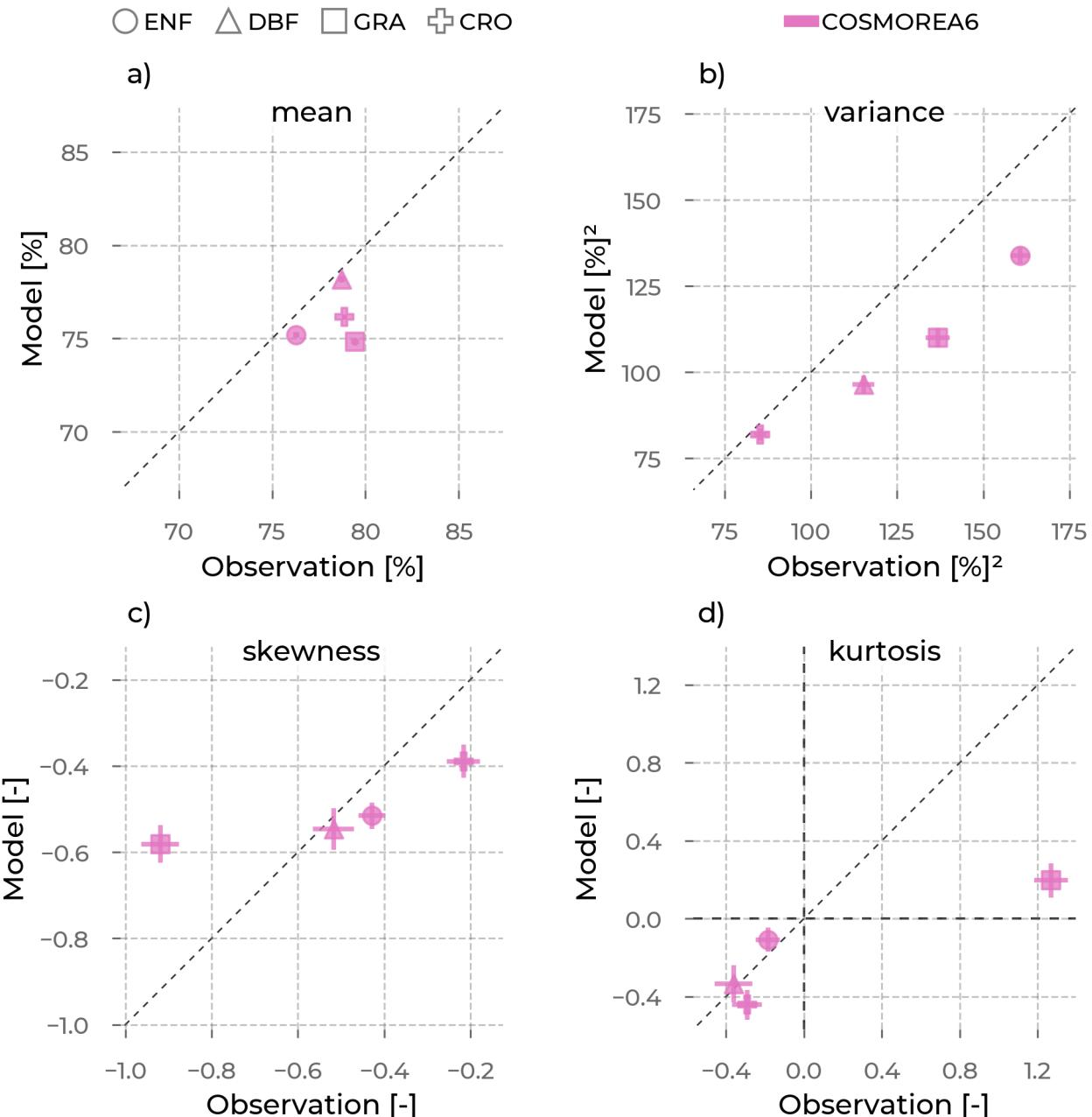
Figure S14: The mean (a), variance (b), skewness (c), and kurtosis (d) of the RH distributions from the models (color, y-axis), as opposed to the corresponding values from observations (x-

axis) aggregated for each PFT (marker type): Evergreen Needleleaf Forest (ENF), Deciduous Broadleaf Forest (DBF), Grasslands (GRA), Croplands (CRO). The error bars are the standard
1315 errors of the respective moment, depending on the sample size.